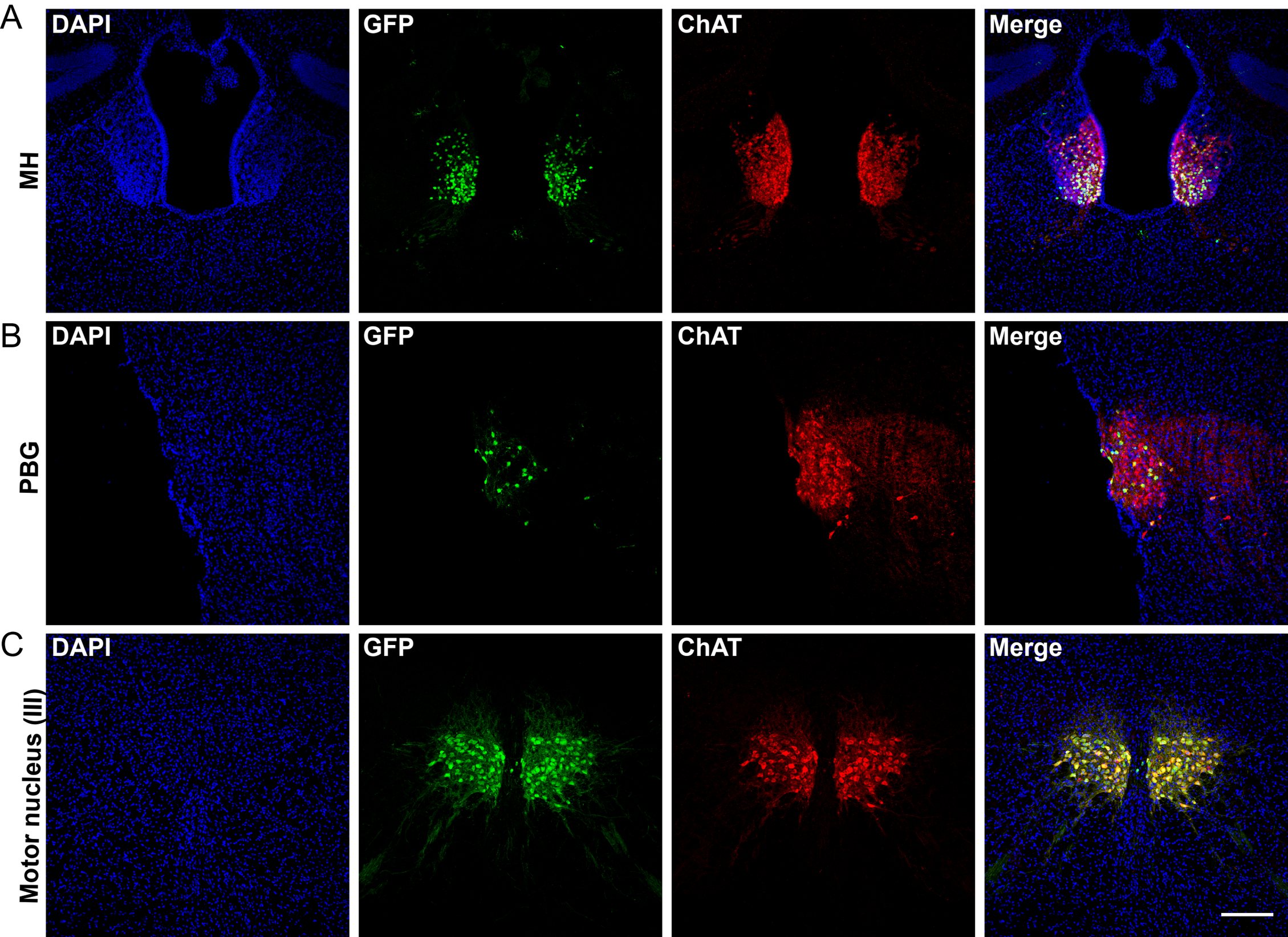
A
DAPI
GFP
ChAT
Merge
MH
B
DAPI
GFP
ChAT
Merge
PBG
C
DAPI
GFP
ChAT
Merge
Motor nucleus (III)

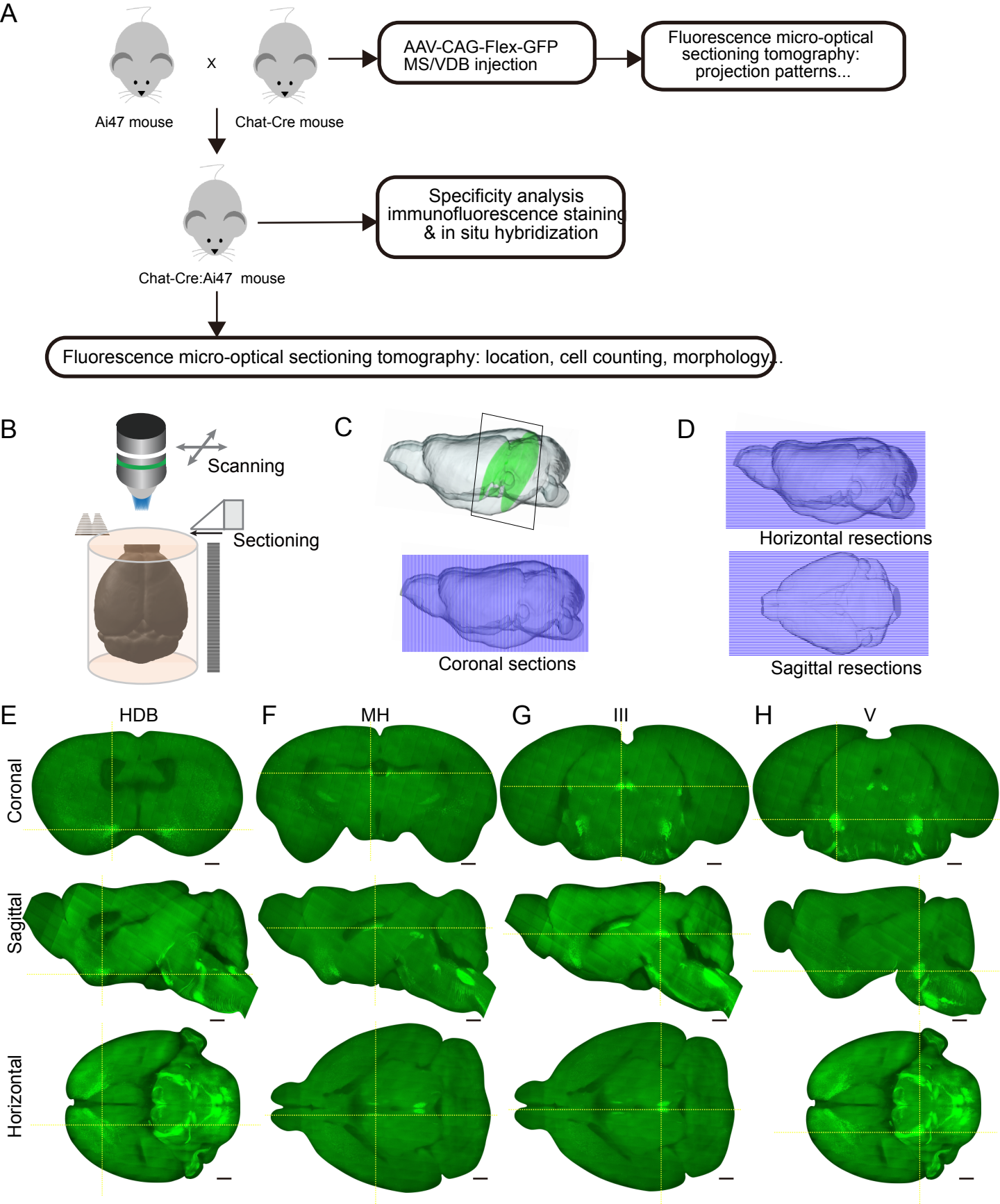
A
Ai47 mouse
X
Chat-Cre mouse
AAV-CAG-Flex-GFP
MS/VDB injection
Fluorescence micro-optical
sectioning tomography:
projection patterns...
Chat-Cre:Ai47 mouse
Specificity analysis
immunofluorescence staining
& in situ hybridization
Fluorescence micro-optical sectioning tomography: location, cell counting, morphology...
B
Scanning
Sectioning
C
Coronal sections
D
Horizontal resections
Sagittal resections
E
HDB
F
MH
G
III
H
V
Coronal
Sagittal
Horizontal

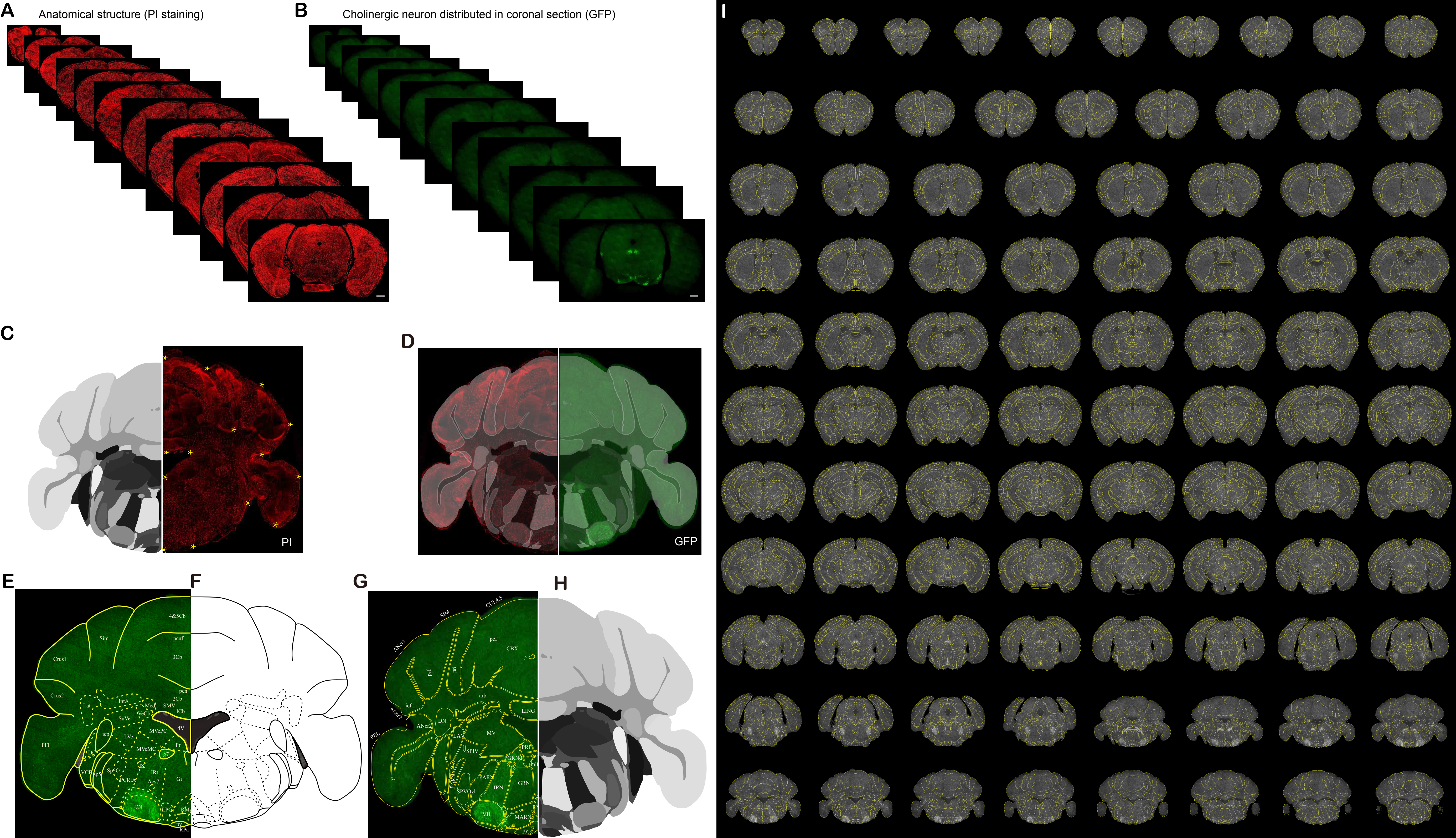
A
Anatomical structure (PI staining)
B
Cholinergic neuron distributed in coronal section (GFP)
C
PI
D
GFP
E
F
G
H
I
Sim
Crus1
Crus2
PFl
SIM
CUL4,5
CBX
VII

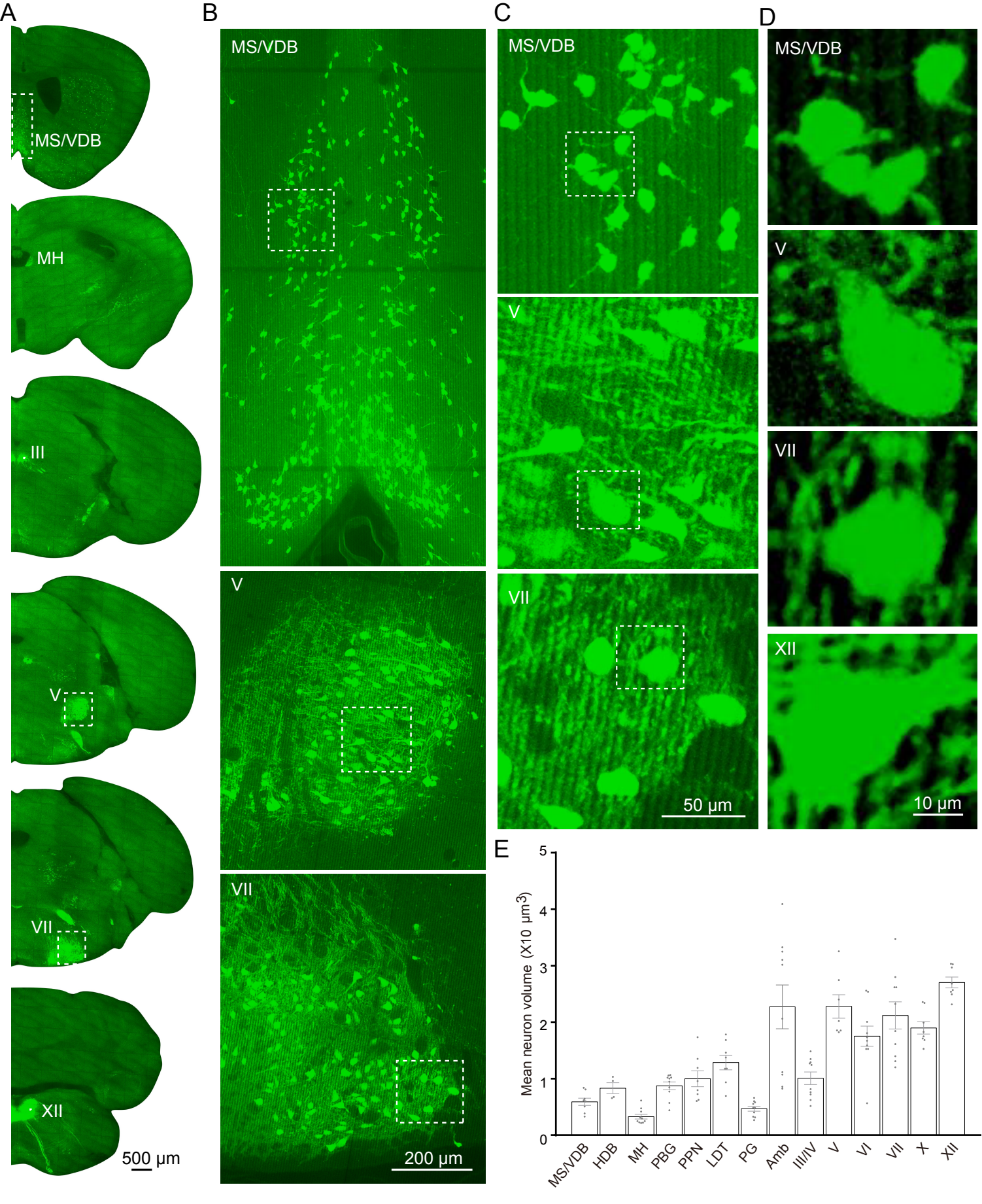
A
MS/VDB
MH
III
V
VII
XII
500 µm
B
MS/VDB
V
VII
200 µm
C
MS/VDB
V
VII
50 µm
D
MS/VDB
V
VII
XII
10 µm
E
Mean neuron volume (X10 µm3)
0
1
2
3
4
5
MS/VDB
HDB
MH
PBG
PPN
LDT
PG
Amb
III/IV
V
VI
VII
X
XII

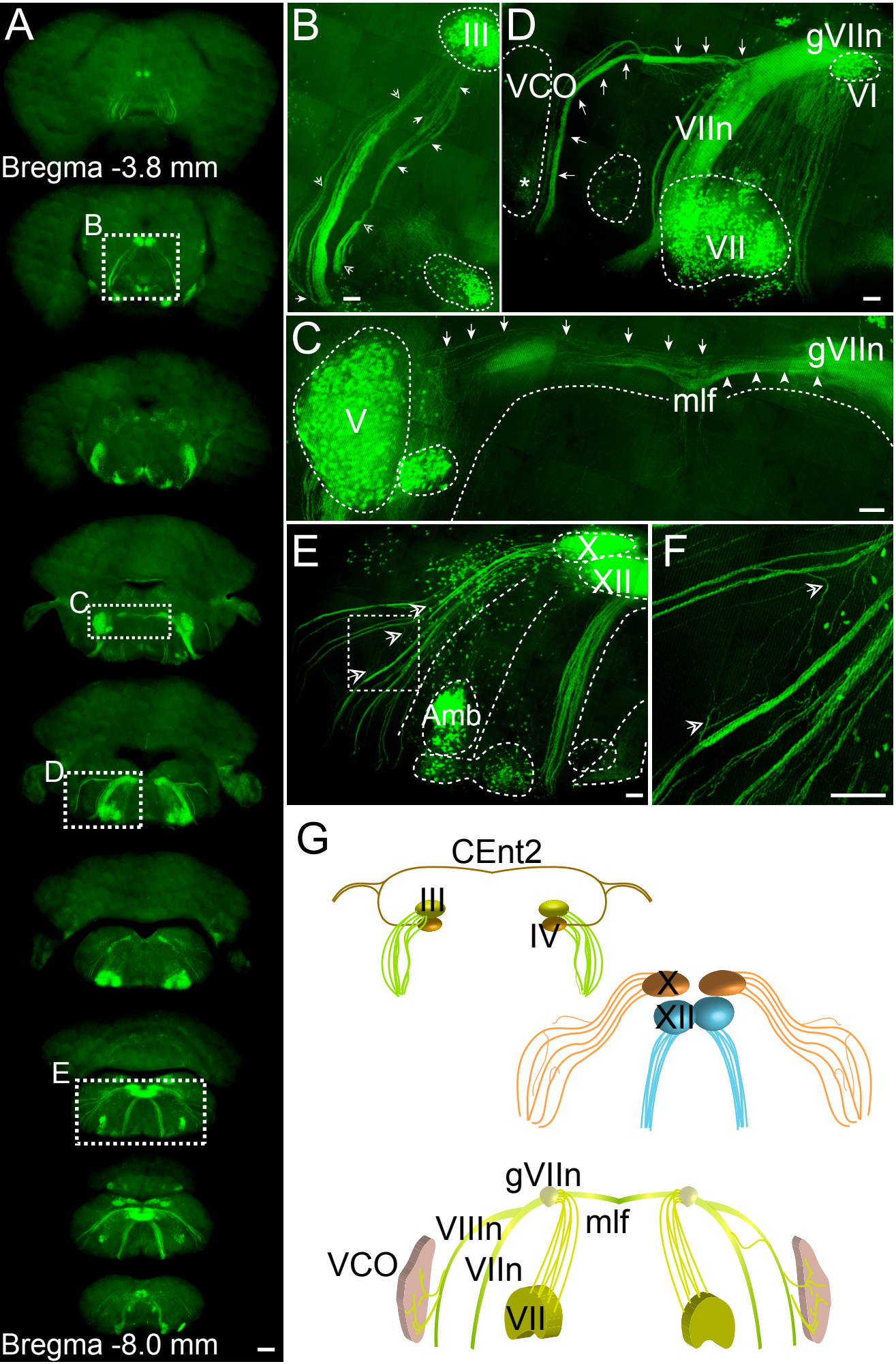
A
Bregma -3.8 mm
B
C
D
E
Bregma -8.0 mm
B
III
D
VCO
gVIIn
VI
VIIn
VII
C
V
gVIIn
mlf
E
X
XII
Amb
F
G
CEnt2
III
IV
X
XII
gVIIn
VIIIn
mlf
VCO
VIIn
VII

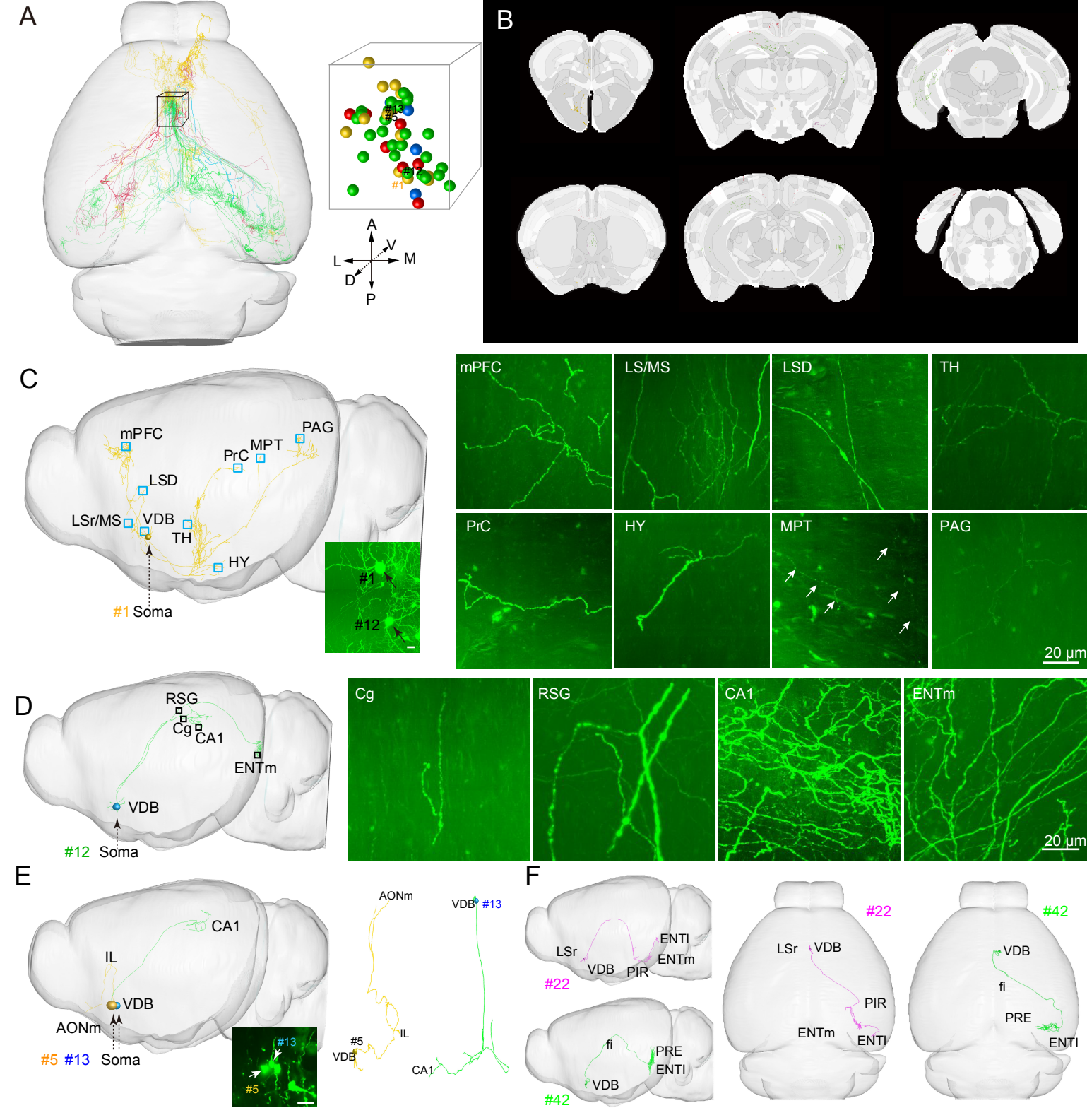
A
#13
#5
#12
#1
A
V
L
M
D
P
B
C
mPFC
PAG
PrC
MPT
LSD
LSr/MS
VDB
TH
HY
#1 Soma
#1
#12
mPFC
LS/MS
LSD
TH
PrC
HY
MPT
PAG
20 μm
D
RSG
Cg
CA1
ENTm
VDB
#12 Soma
Cg
RSG
CA1
ENTm
20 μm
E
CA1
IL
VDB
AONm
#5 #13 Soma
#13
#5
AONm
VDB #13
#5
IL
VDB
CA1
F
LSr
ENTl
VDB
ENTm
PIR
#22
fi
PRE
ENTl
VDB
#42
#22
LSr
VDB
PIR
ENTm
ENTl
#42
VDB
fi
PRE
ENTl

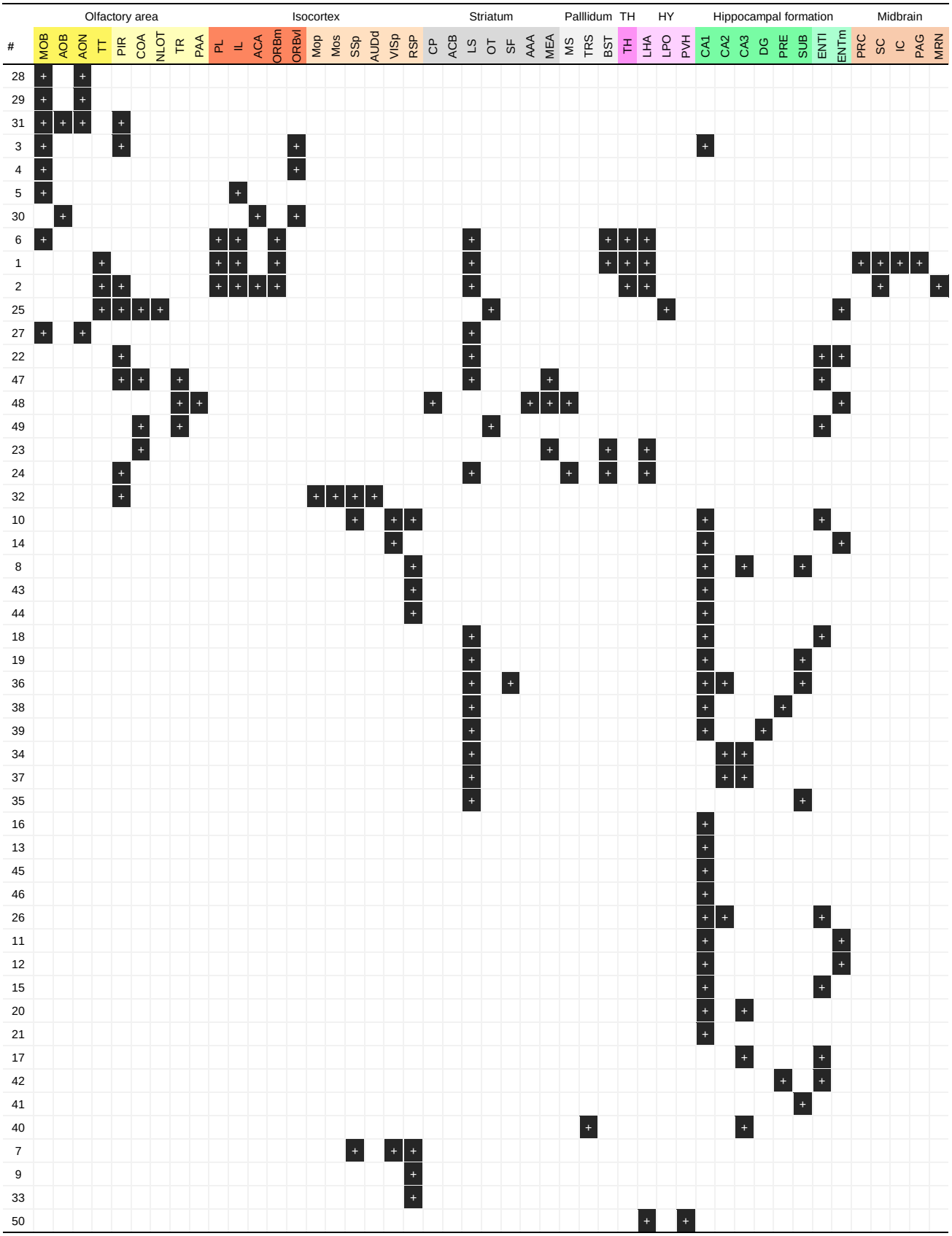
Olfactory area
Isocortex
Striatum
Palllidum
TH
HY
Hippocampal formation
Midbrain
#
MOB AOB AON TT PIR COA NLOT TR PAA PL IL ACA ORBm ORBvl Mop Mos SSp AUDd VISp RSP CP ACB LS OT SF AAA MEA MS TRS BST TH LHA LPO PVH CA1 CA2 CA3 DG PRE SUB ENTl ENTm PRC SC IC PAG MRN
28
29
31
3
4
5
30
6
1
2
25
27
22
47
48
49
23
24
32
10
14
8
43
44
18
19
36
38
39
34
37
35
16
13
45
46
26
11
12
15
20
21
17
42
41
40
7
9
33
50

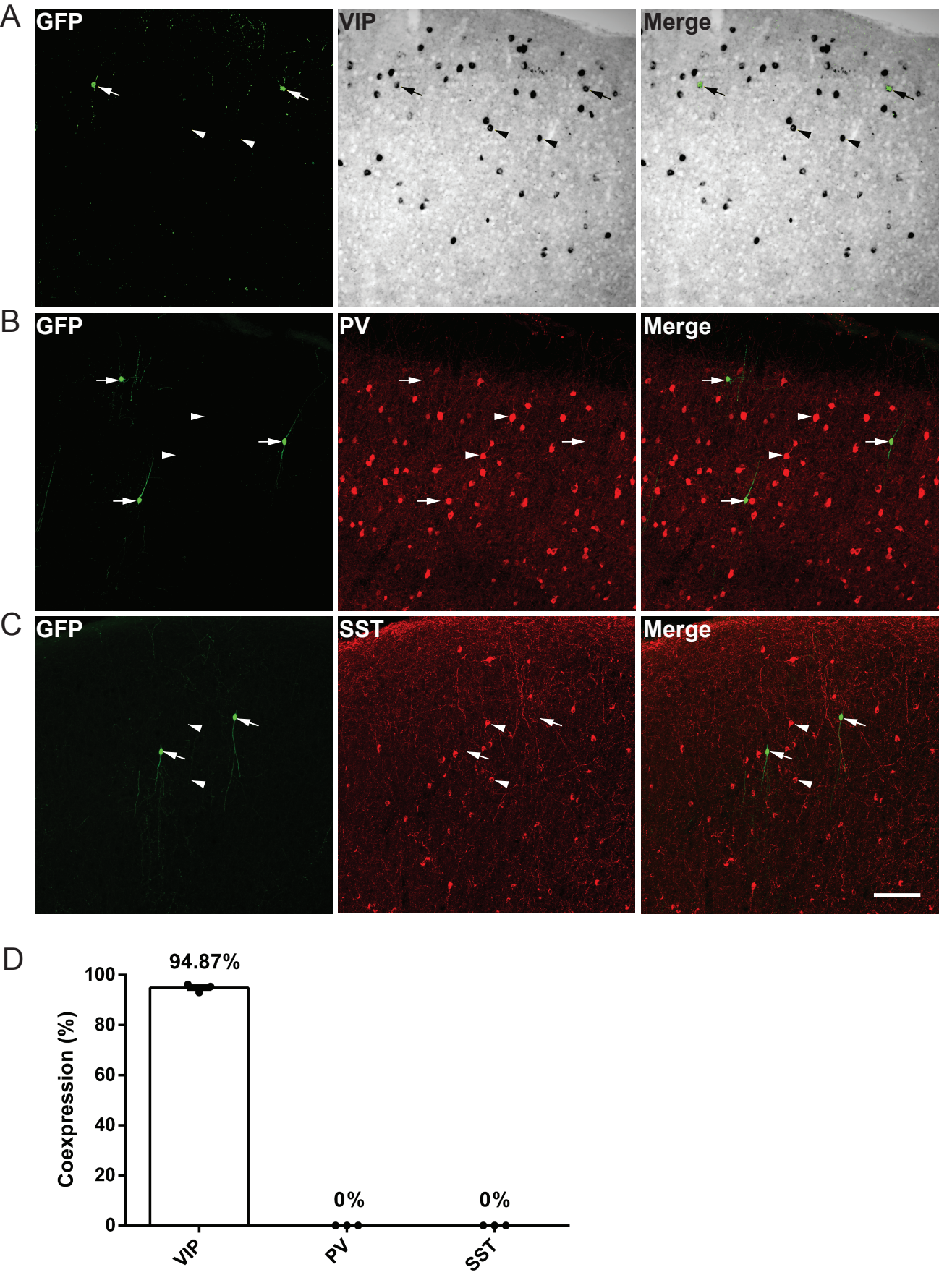
A
GFP
VIP
Merge
B
GFP
PV
Merge
C
GFP
SST
Merge
D
94.87%
100
80
60
40
20
0
Coexpression (%)
0%
0%
VIP
PV
SST

Table S1. Colocalization (percentage of GFP positive neurons expressing ChAT) and labeling ratios (percentage of ChAT positive neurons expressing GFP) of Chat-Cre:Ai47 mice in different brain regions.

Brain region	Mouse NO.	GFP+ NO.	ChAT+ NO.	Colocalization (%)	Labeling (%)
MOp	3	65	241	92.31	24.90
MOs	3	39	159	89.74	22.01
mPFC	3	26	65	96.15	38.46
SSp	3	101	294	98.02	33.67
VISp	3	65	228	89.23	25.44
MS/VDB	3	876	1256	89.04	65.90
Striatum	3	807	787	96.41	98.86
PPN	3	539	667	95.92	77.51
LDT	3	1034	1426	94.49	68.51

Table S2. Number of cholinergic neurons in 22 brain regions.

	Number of cholinergic neurons	**s.e.m**
mPFC	73	13
MOp	178	22
MOs	163	21
SSp	330	18
VISp	169	21
HPF	53	11
ARH	42	7
DMH	71	4
MS/VDB	1665	178
HDB	3123	238
MH	2732	183
III/IV	673	55
PBG	268	39
PG	2039	220
V	1060	46
VI	136	9
LDT	574	28
PPN	578	50
VII	2993	161
Amb	392	33
X	1947	78
XII	1885	41

Table S3. Soma volume of cholinergic neurons in 14 brain regions.

	Cholinergic neuron volume (μm^3)	**s.e.m**
MS/VDB	596.73	54.27
HDB	840.12	53.36
MH	330.32	40.29
PBG	882.51	65.99
PPN	1009.05	119.32
LDT	1299.56	109.65
PG	471.78	40.86
Amb	2296.85	372.11
III/IV	1017.69	106.81
V	2303.76	163.09
VI	1770.65	171.69
VII	2142.78	230.37
X	1919.34	91.91
XII	2732.71	81.75

Table S4. Co-expression ratios of GFP (Chat-ires-Cre:Ai47) and primary interneuron markers (in situ hybridization or immunofluorescence staining) in the cortex.

Interneuron marker	Mouse NO.	GFP+ NO.	Colocalization(%)
VIP	3	139	94.87
PV	3	127	0
SST	3	112	0

Table S5. The percentage of cholinergic neurons in L2/3 and L4-6 in different cortical regions.

	L2/3	s.e.m		L4-6	s.e.m
mPFC	88.70661	3.233957	**mPFC**	11.29339	3.233957
M1	73.56727	1.252281	**M1**	26.43273	1.252281
M2	83.73701	1.141685	**M2**	16.26299	1.141685
S1	84.24741	1.751588	**S1**	15.75259	1.751588
V1	95.95534	1.056959	**V1**	4.044663	1.056959

Table S6. Abbreviation for brain area.

AAA	Anterior amygdalar area	MH	medial habenula
ACA	Anterior cingulate area	mlf	medial longitudinal fascicle
ACB	Nucleus accumbens	MOB	Main olfactory bulb
aco	anterior commissure, olfactory limb	MOp	primary motor area
AM	anteromedial nucleus of thalamus	MOs	secondary motor area
Amb	nucleus ambiguus	mPFC	medial prefrontal cortex
AOB	Accessory olfactory bulb	MRN	midbrain reticular nucleus
AON	Anterior olfactory nucleus	MS	medial septal nucleus
AONm	anterior olfactory nucleus, medial part	NLOT	Nucleus of the lateral olfactory tract
ARH	arcuate hypothalamic nucleus	ORBm	Orbital area, medial part
AUDd	Dorsal auditory area	ORBvl	Orbital area, ventrolateral part
BST	Bed nuclei of the stria terminalis	OT	Olfactory tubercle
CA1	Field CA1	PAA	Piriform-amygdalar area
CA2	Field CA2	PAG	periaqueductal gray
CA3	Field CA3	PBG	parabigeminal nucleus
cc	corpus callosum	PG	pontine grey
COA	Cortical amygdalar area	PIR	Piriform area
CP	Caudoputamen	PL	Prelimbic area
df	dorsal fornix	PPN	pedunculopontine nucleus
DG	Dentate gyrus	PRC	Precommissural nucleus
dhc	dorsal hippocampal commissure	PRE	Presubiculum
DMH	dorsomedial nucleus of hypothalamus	PVH	Paraventricular hypothalamic nucleus
ENTl	Entorhinal area, lateral part	RSP	Retrosplenial area
ENTm	entorhinal area, medial part	SC	Superior colliculus
Epv	Endopiriform nucleus, ventral part	SF	Septofimbrial nucleus
fi	fimbria	SSp	primary somatosensory area
gVIIN	genu of facial nerve	SUB	Subiculum
HDB	the horizontal limb of diagonal band nucleus	TH	Thalamus
HPF	hippocampal formation	TR	Postpiriform transition area
IC	Inferior colliculus	TRS	Triangular nucleus of septum
III	oculomotor nucleus	TT	Taenia tecta
IL	Infralimbic area	V	motor nucleus of trigeminal
IV	trochlear nucleus	VCO	ventral cochlear nucleus
LDT	laterodorsal tegmental nucleus	VDB	the vertical limb of diagonal band nucleus
LHA	Lateral hypothalamic area	VI	abducens nerve
lot	lateral olfactory tract, body	VII	facial motor nucleus
LPAG	lateral periaqueductal gray	VIIIn	vestribular nerve
LPO	Lateral preoptic area	VIIn	facial nerve
LS	Lateral septal nucleus	VISp	Primary visual area
MD	mediodorsal nucleus of thalamus	X	dorsal motor nucleus of vagus
MEA	Medial amygdalar nucleus	XII	hypoglossal nucleus

Supplementary Text

Supplementary Materials and Methods

Genetically modified mice

Chat-ires-Cre mice (018957) were obtained from the Jackson lab. The use and care of animals complied with the guidelines of the Animal Advisory Committee at the Shanghai Institutes for Biological Science, CAS. The raw data are publicly available on our lab homepage for the Visible Brain-wide Networks project: http://vbn.org.cn/. The original-resolution images are available upon request on a hard drive.

Construction of Ai47 mice

In the Ai47 mouse line, the Rosa26 locus has been modified by targeted insertion of a construct containing the strong and ubiquitously active CAG promoter, a loxP-flanked stop cassette, a triple GFP gene unit, a woodchuck hepatitis virus posttranscriptional regulatory element (WPRE) and a polyA signal. The triple GFP unit was generated by gene synthesis (GenScript Corp.) and contains sequences for Emerald-GFP (Life Technologies), TagGFP2 (Evrogen) and humanized Renilla GFP variants, which were linked together by viral T2A and P2A oligopeptide sequences. The Ai47-targeting construct was transfected into the 129S6B6F1 hybrid ES cell line G4, and correctly targeted clones were identified by PCR and Southern blotting and then injected into C57BL/6J blastocysts to obtain chimeras for eventual germline breeding. The resulting mice were crossed with the Rosa26-PhiC31 line (JAX Stock #007743) to delete the

PGK-Neo selection cassette through PhiC31-mediated recombination between the AttB and AttP recombinase sites in the germline of the mice. Ai47 mice were crossed with *Chat-ires-Cre* mice, and the double-positive mice (3-6 months old) were used in the present study.

Virus injection

Recombinant adeno-associated virus (AAV-CAG-FlEX-GFP, Serotype: 9, UNC Gene Therapy Center Vector Core, Chapel Hill, NC, USA) was used as the anterograde tracer in 2-month-old *Chat-ires-Cre* mice. A total of 80 nL of virus was injected using a pressure injector (Nanoject II; Drummond Scientific Co., Broomall, PA, USA). The stereotaxic coordinates for the target area were based on the Mouse Brain in the Stereotaxic Coordinates atlas. For NDB, the injection site was set to 0.98 mm A-P, 0 mm medial-lateral (M-L), and 4.8 mm dorsal-ventral (D-V). The mice recovered quickly after surgery and survived 28 days before euthanasia.

Tissue preparation

All histological procedures have been described previously(1-4).

Briefly, for whole-brain imaging, the mice were anesthetized and perfused with 0.01 M PBS (Sigma-Aldrich Inc., St. Louis, US), followed by 4% paraformaldehyde (PFA) and 2.5% sucrose in 0.01 M PBS. The brains were postfixed in 4% PFA for 24 h. After fixation, each intact brain was rinsed and subsequently dehydrated via immersion in a graded ethanol series. Then, each brain was impregnated with Glycol Methacrylate

(GMA, Ted Pella Inc., Redding, CA) and embedded in a vacuum oven.

For AAV/RV-tracing experiments, the mice were perfused with PBS followed by PFA. After post-fixation in PFA, consecutive 75-μm coronal sections were collected using a cryostat (Leica VT1200), washed 3 × 20 min with PBS, and stained with DAPI (1:10000 of 5 mg/ml, Sigma-Aldrich), which was included in the last PBS wash. Slides were cover-slipped. Samples were imaged using a Zeiss LSM 710 confocal microscope (Carl Zeiss, LSM710).

Instrument

As described in our previous work (4), the whole-brain imaging system consists of three parts: a structured-illumination microscope, a microtome and the control system. The light source is a mercury lamp with high flexibility in wavelength selection. A high-precision 3D translation stage moves the sample, while a diamond knife (DIATOME) is used on the microtome to remove the imaged sections. The control system is divided into a data acquisition portion and a motion control portion for robustness considerations.

Whole-brain imaging

Our previous work showed that the GMA formulation improves fluorescence preservation of EGFP-labeled neurons nearly twofold if the solution pH is alkaline (2, 3). To preserve the fluorescence of EGFP during whole-brain imaging, the embedded sample was placed in a 0.01 M Na_2CO_3 solution. The whole-brain sample was

immobilized in an antero-posterior (A-P) direction in the water bath on the 3D translation stage. When these imaging parameters are set, the whole-brain imaging system performs the sectioning and imaging process automatically to complete the brain-wide dataset acquisition.

The dataset, consisting of 1700 × 1800 pixel-sized tiles, was saved at 16-bit depth in a LZW-compression TIF format. After collection, we sent the entire dataset to a PB-sized distributed storage by way of a standard 10-Gigabit fiber.

Image processing

Image processing was performed based on our previously developed algorithm (1, 4-6). Image preprocessing is implemented in C++, parallel-optimized with Intel MPI Library (v3.2.2.006), and executed on a computing server. Following preprocessing, we imported the standard dataset to Amira software (v5.2.2, Mercury Computer Systems, San Diego, CA, USA) for visualization on desktop graphical workstations. Almost all figures and movies were obtained with basic operations in Amira and Fiji, including extracting the interesting regions, resampling or interpolation, maximum-intensity projection, volume rendering, moviemaker with the main module, man-machine interactive with Filament editor and with segmentation editor, etc. Briefly, the dataset acquired by the dual-color precise imaging system was separated into the GFP and PI channels. The PI-labeled data set was imported into Amira to manually generate the outline of the mouse brain.

Cholinergic neuron characterizations were calculated with Amira, Imaris software

(Bitplane AG, Zurich) and NeuroGPS software (7). Briefly, NeuroGPS software was used to count the GFP-labeled neurons in the whole brain. Before calculation of the volume of each neuron, preprocessing was performed, including isolating the dataset for the chosen brain regions with Amira software. Imaris software was used to quantify the neuron volume. In addition, we calculated the volume of selected regions using Amira software. Data from both brain hemispheres were used here.

To distinguish the brain regions, we aligned the whole-brain dataset to the Allen Reference Atlas according to previous studies (5, 6). Here, we used the Common Coordinate Framework V3 (the 3rd version of the Allen Reference Atlas, abbreviated as CCF)(8), as the registration template. For this Framework, the resolution was 10 × 10 × 10 μm. We down-sampled the raw data from the PI-staining results from 0.32 × 0.32 × 2 μm to 10 × 10 × 10 μm. Then, we manually segmented the cytoarchitectural information of several brain regions as landmarks. Finally, we registered the figures of the GFP channel to the results of the PI channel. Then, we loaded the outline of mouse brain and the tracing results into Amira simultaneously and used the moviemaker module of Amira to generate movies.

When analyzing the projection patterns in the whole brain, we performed an affine transformation and a symmetric image normalization (9-11) in Advanced Normalization Tool (10, 12) to achieve the 3D co-registration of the PI-stained dataset with the Allen template dataset. Three skilled technicians independently performed back-to-back manual validation and amendment in Amira software, followed by cross-validations.

Cholinergic neuron reconstruction and morphological analysis

Following a previous procedure (4), the reconstructions of the cortical cholinergic neurons was completed interactively in Amira visualization and data analysis software (Visage Software, San Diego, CA). In Amira, the whole-brain dataset was converted into a large-disk data object, and the fibers in each sub-volume were traced interactively. The reconstructed neurons were checked back-to-back by 3 persons.

The morphologies of cholinergic neurons were highly diverse. We traced 50 individual cholinergic neurons in the vertical limb of the diagonal band nucleus. The locations of the soma and every axonal terminal were distinguished in the aligned dataset of the whole brain. Cortical cholinergic neurons were reconstructed and then classified based on their soma and dendritic geometry (thickness, bifurcation, angle, branching order) (13). Bipolar cells (BPCs) have narrow bipolar dendrites extending to L1 and L6. Bitufted cells (BTCs) have two bundles of vertically oriented dendrites with a bitufted morphological pattern. Double bouquet cells (DBCs) have a narrow, bitufted dendritic tree. Multi-polar neurons have multi-polar dendrites that form spherical dendritic fields. We compared the lengths and branch numbers of the dendrites of neurons in different layers of M1, V1 and S1.

Histology and image analysis

For immunohistochemical staining, adult *Chat-ires-Cre*:Ai47 mice (2-6 months old) were perfused with PBS followed by 4% PFA in phosphate buffer. The brain was

extracted and postfixed in 4% PFA for 4 h at 4 °C. Dehydration was performed in 30% sucrose in PBS, and coronal brain slices at 50-μm thickness were prepared using a vibratome (Leica, CM1950). Brain slices were blocked for 1 h at room temperature in PBS-T (0.3% Triton X-100) with 5% bovine serum albumin, fraction V. The primary antibodies used were goat anti-ChAT (Millipore, AB144P, 1:400), mouse anti-PV (Millipore, MAB1572, 1:1000), goat anti-SST (Santa Cruz, sc-7819, 1:250), and rabbit anti-GFP (Invitrogen, A11122, 1:1000). The secondary antibodies used were donkey anti-goat IgG Alexa 555 (Invitrogen, A21432, 1:1000), donkey anti-mouse IgG Alexa546 (Life technologies, A10036, 1:1000), and donkey anti-rabbit IgG Alexa488 (Life technologies, A21206, 1:1000). For VIP in situ hybridization, experiments were performed according to standard methods. VIP sense and anti-sense probes were chosen from the Allen Brain Atlas at www.brain-map.org. All images were acquired on a Nikon TiE-A1 plus confocal microscope, and cell counting was carried out manually using ImageJ.

Statistical analysis

Statistical significance was analyzed using GraphPad Prism. All measurements are listed as the mean ± s.e.m. Statistical comparisons were performed using Student's t-test and ANOVA.

Reference:

1. Gong H, Zeng S, Yan C*, et al.* (2013) Continuously tracing brain-wide long-distance axonal projections in mice at a one-micron voxel resolution. *NeuroImage* 74:87-98.

2. Yang Z, Hu B, Zhang Y*, et al.* (2013) Development of a plastic embedding method for large-volume and fluorescent-protein-expressing tissues. *PloS one* 8(4):e60877.
3. Xiong H, Zhou Z, Zhu M*, et al.* (2014) Chemical reactivation of quenched fluorescent protein molecules enables resin-embedded fluorescence microimaging. *Nature communications* 5:3992.
4. Gong H, Xu D, Yuan J*, et al.* (2016) High-throughput dual-colour precision imaging for brain-wide connectome with cytoarchitectonic landmarks at the cellular level. *Nature communications* 7:12142.
5. Peng J, Long B, Yuan J*, et al.* (2017) A Quantitative Analysis of the Distribution of CRH Neurons in Whole Mouse Brain. *Frontiers in neuroanatomy* 11(63).
6. Li Y, Gong H, Yang X*, et al.* (2017) TDat: An Efficient Platform for Processing Petabyte-Scale Whole-Brain Volumetric Images. *Frontiers in neural circuits* 11.
7. Quan T, Zhou H, Li J*, et al.* (2016) NeuroGPS-Tree: automatic reconstruction of large-scale neuronal populations with dense neurites. *Nature methods* 13(1):51-54.
8. Kuan L, Li Y, Lau C*, et al.* (2015) Neuroinformatics of the Allen Mouse Brain Connectivity Atlas. *Methods* 73:4-17.
9. Rueckert D, Sonoda LI, Hayes C*, et al.* (1999) Nonrigid registration using free-form deformations: application to breast MR images. *IEEE Trans Med Imaging* 18(8):712-721.
10. Klein A, Andersson J, Ardekani BA*, et al.* (2009) Evaluation of 14 nonlinear deformation algorithms applied to human brain MRI registration. *NeuroImage* 46(3):786-802.
11. Ni H, Ren M, Zhong Q*, et al.* (2015) Co-registration of diffusion tensor imaging and micro-optical imaging based on ants.
12. Avants BB, Tustison NJ, Song G*, et al.* (2011) A reproducible evaluation of ANTs similarity metric performance in brain image registration. *NeuroImage* 54(3):2033-2044.
13. Jiang X, Shen S, Cadwell CR*, et al.* (2015) Principles of connectivity among morphologically defined cell types in adult neocortex. *Science* 350(6264):aac9462.

Supplementary Figure Legends

Supplementary Figure 1. Analysis of expression specificity of *Chat-ires-Cre*:Ai47 mice in the MHb, PBG and motor nucleus.

A. In the MHb, almost all GFP-positive neurons were ChAT positive, and the number of ChAT-positive neurons was far higher than the number of GFP-positive neurons. B. As in the MH, almost all GFP-positive neurons were ChAT positive, and ChAT-positive neurons vastly outnumbered GFP-positive neurons, in the PBG. C. In the oculomotor nucleus (III), GFP and ChAT showed precise co-labeled. Scale bar: 100 μm.

Supplementary Figure 2. Whole-brain imaging of the cholinergic neurons.

A. Workflow of the Cre-dependent AAV injection approach. B. Diagram of the whole-brain imaging procedure in the brain positioning system. C. All coronal sections were self-segmented, and their figures were used for reconstruction of the whole brain in 3D. D. The whole-brain dataset can be re-sectioned at any angle (horizontal, sagittal, etc.). (E-H) Coronal, sagittal and horizontal views of GFP-labeled neurons showed the distribution of neurons in the HDB, MH, III and V nuclei.

Supplementary Figure 3. Cholinergic neuron distribution in sagittal sections.

A. PI was applied to the imaging buffer for real-time staining to dissect the anatomical structure while detecting the GFP signals. Continuous coronal sections taken at 500-μm intervals showed PI-stained slices from a mouse brain. The thickness of the section was 2 μm. B. Corresponding coronal sections are maximum-intensity projection showing GFP-labeled cholinergic neurons in the entire mouse brain. The thickness of the projection was 50 μm. Scale bar: 500 μm. C. Registration of raw images onto

corresponding coronal sections of the Allen Reference Atlas. The registration module applied several geometric transformations of the raw PI-staining image to optimize the match of reference points between the raw image and atlas. D. The GFP-channel image was registered to the Allen Reference Atlas with the reference points in the PI-staining image. E, F. The raw data of coronal sections were registered to the Paxinos brain atlas. G, H. the raw data were registered to the Allen Common Coordinate Framework (http://mouse.brain-map.org/static/atlas). I. The continuous coronal sections of the whole-brain dataset were aligned to the Allen Framework. The yellow lines show the edge of the brain region.

Supplementary Figure 4. Soma volumes of cholinergic neurons in subcortical nuclei.

A. Images of 6 sections showing the architectonic structure of subcortical regions in the whole brain. Scale bar: 500 μm. B. Illustration of cholinergic neurons in MS/VDB, V and VII nuclei. Scale bar: 200 μm. C. Magnified view showing neuronal soma in different regions. Scale bar: 50 μm. D. Cell bodies of cholinergic neurons in the boxed area in (C), including MS/VDB, MH, III, V, VI, VII and XII nuclei. Scale bar: 10 μm. E. Soma volumes of cholinergic neurons in 14 sub-regions of a single hemisphere (n = 10 from 5 brains).

Supplementary Figure 5. Axonal projections of cholinergic neurons in midbrain and brainstem.

A. Coronal sections showed cholinergic nuclei in midbrain and brainstem. Every image is the preview of the maximum intensity projection that the thickness is 500 μm. B-F. Magnified views of the regions in A showed an aggregate distribution of cholinergic neurons in III, V, VI, VII, X and XII while some of their axonal projections arrayed in slender bands. B. The solid arrow showed where the branches of III separated from the bundles of axonal fibers. The hollow arrowheads labeled where the axonal fibers re-access in the bundles of nerve fiber. C. the arrows with tail showed the axonal projection from V to the ipsilateral area through mlf and the arrows without tail showed the ipsilateral fibers to gVIIn. D. The arrows showed the branches from VIIn and projected to VCO. The star showed the terminal in VCO from the branches. E. The projections of X divided in many bundles with some fibers crossed between different bundles. F. The large view of labeled part in E. G. The diagram showed the different projections patterns of the cholinergic neurons in these motor nuclei.

Supplementary Figure 6. 3D distribution of cholinergic neurons in the MS/VDB and the axon arbors of the reconstructed neurons.

A. Horizontal view of the 50 reconstructed neurons and the distribution of neuronal soma. The soma of individual neurons were labeled with four colors: green for those that mainly project to the hippocampal formation, yellow for those that mainly project to the olfactory area, red for those that mainly project to non-cortical olfactory areas, and blue for those that mainly project to cortex and other areas. B. Serial coronal sections aligned to the Allen Framework showing the axonal locations of the

reconstructed neurons. C. 3D view of the #1 neuron and the details of the axon arbors in different areas. The insert figure is a maximum-intensity projection (thickness: 100 μm) of the coronal section showing the location of #1 and #12. D. 3D view of the #12 neuron and the details of the axon arbors in different areas. E. 3D view of the #5 neuron and #13 neuron located in VDB and the details of the axon arbors in different areas. The inset fluorescence image is raw data from the coronal section (thickness: 2 μm) showing the location of the neurons (#5 and #13). F. Horizontal and sagittal view of neurons (#22, #42) that project to different areas.

Supplementary Figure 7. Co-expression profile of interneuron markers and GFP (*Chat-ires-Cre*:Ai47) in cortex.

A．In situ hybridization showing that GFP+ neurons mostly co-expressed VIP. Arrows, GFP and VIP co-expressing neurons; arrowheads, VIP-positive neurons. B, C. Immunofluorescence staining showing that almost all GFP+ neurons were PV and SST negative. Arrows, GFP-positive neurons; arrowheads, PV- or SST-positive neurons. Scale bar, 100 μm. D. Statistical results of co-expression profile. Error bar: s.e.m. n = 3 mice.